Chinese Chemical Letters 34 (2023) 108241

Contents lists available at ScienceDirect

Chinese Chemical Letters

journal homepage: www.elsevier.com/locate/cclet

Recent advances in MXenes-based glucose biosensors

Shunyao Tian[a], Meng Wang[a], Paolo Fornasiero[b,c], Xiaoyu Yang[d], Seeram Ramakrishna[e], Shih-Hsin Ho[a], Fanghua Li[a,*]

[a] State Key Laboratory of Urban Water Resource and Environment, School of Environment, Harbin Institute of Technology, Harbin 150090, China
[b] Department of Chemical and Pharmaceutical Sciences, University of Trieste, Via L. Giorgieri 1, Trieste 34127, Italy
[c] Consorzio Interuniversitario Nazionale per la Scienza e Tecnologia dei Materiali (INSTM), Unit of Trieste, via L. Giorgieri 1, Trieste 34127, Italy
[d] School of Chemical and Environmental Engineering, China University of Mining and Technology, Beijing 100083, China
[e] Center for Nanotechnology and Sustainability, Department of Mechanical Engineering, National University of Singapore, Singapore 119077, Singapore

ARTICLE INFO

Article history:
Received 10 September 2022
Revised 28 January 2023
Accepted 16 February 2023
Available online 19 February 2023

Keywords:
MXenes
Biosensor
Mechanism
Blood glucose
Glucose detection

ABSTRACT

It is established that monitoring blood glucose on a daily basis is one of the most effective solutions to prevent and treat diabetes. Consequently, developing a glucose sensing platform with outstanding sensing performance occupies an indispensable position for the early diagnosis and risk assessment of diabetes. Recently, biosensor has been deemed as a promising apparatus to acquire the signals for glucose monitoring based on 2D materials. However, it is unsatisfied to deploy some materials widely as a result of some inherent defects. Carbon nanotubes have comparatively high toxicity. MoS_2 with unfavourable biocompatibility are still arduously implemented on being functionalized. Fortunately, MXene, a brand-new and rapidly developing two-dimensional material, exhibits marvellous application potential in the domain of biosensing. Therefore, it has exerted tremendous attention from diverse scientific fields owning to its remarkable properties, such as excellent hydrophilicity, metal-like conductivity, abundant surface functional groups, unique layered structure, large specific surface area and remarkable biocompatibility. This review mainly focuses on the main synthetic route of MXenes, as well as the recent advancements of biosensors involving MXenes as an electrode modifier for glucose detection. In addition, the promising prospects and challenges of glucose sensing technology based on MXenes are also discussed.

1. Introduction

As one of the most serious non-communicable diseases in the world [1], diabetes haunts hundreds of millions of people globally. According to the IDF Diabetes Atlas 2021 reports published by the International Diabetes Federation, the number of adults with diabetes worldwide will reach 537 million (10.5%) in 2021 [2], an increase of 74 million in two years compared to 2019 [2]. Videlicet, about one in ten adults worldwide suffers from diabetes. According to the IDF, the number will reach 783 million by 2045 [3]. It means a 46% increase that is more than twice the estimated population growth (20%) during the same period, plaguing one in eight adults [2]. This serious disease, marked by elevated glucose levels in the blood, is caused by insufficient insulin secretion produced by the pancreas or ineffective use of insulin. And it will lead to a series of serious complications that cause serious damage to the human body or even death, including diabetic foot ulcer, diabetic glomerulosclerosis, lactic acidosis and cardiovascular complications in the absence of appropriate. Therefore, the development of a blood glucose detection system with greater accuracy and sensitivity stands out for the risk assessment, early diagnosis, and possibility of successful treatment.

As a significant component of blood glucose detection system, glucose biosensor plays a vital role as an indispensable tool for medical diagnosis. The general working principle of biosensors can be summarized as follows [4]: (1) differentiate and detect the required biomarker in the real blood environment, (2) convert this biological signal into a measurable signal (such as electrical signals), then (3) process the converted signal through an amplifier to simplify the relevant operations in practical situations.

As the research on MXenes nanomaterials have become a hot spot, mounting numbers of glucose biosensors with high sensitivity, wide detection range, excellent thermal stability and reliable selectivity have been reported continuously [5]. The introduction of MXenes will significantly improve the performance of glucose sensors and bring subversive and revolutionary developments to related research [4].

* Corresponding author.
E-mail address: fanghuahope99@outlook.com (F. Li).

https://doi.org/10.1016/j.cclet.2023.108241
1001-8417/

MXenes is a general term for a large class of emerging 2D nanosheet materials, including transition metal carbides, nitrides and carbonitrides [6–9]. Since Prof. Gogotsi's research team discovered and named MXenes for the first time in 2011 [10], this graphene-like 2D material with unique properties and abundant surface activity has been captured attention. The precursor of MXenes is MAX, which can be represented by $M_{n+1}AX_n$ ($n = 1$, 2 or 3). In this expression, M represents a sequence of early transition metal such as Ti, Zr, Ta, Nb and Mo [11]. A can be described as elements of 13-16 groups [12], and X represents C, N or C/N [13]. In the MAX phase, the atomic layers of M and X are arranged to form a compact hexagonal structure. In addition, X occupies the octahedral void, where the chemical coefficient of the main group element A is higher. And the bond energy of M-A is significantly lower than that of M-X [14]. This ternary carbon or nitride monolayer nanosheet $M_{n+1}X_nT_x$ is obtained by selectively etching off the A layer in the 3D MAX phase and then separating it with ultrasound [12], where "ene" refers to its graphene-like properties [15]. Notably, the surface functional groups T_x of MXenes obtained with etchants are usually fluorine (-F), hydroxide (-OH) and oxygen (-O). Thus, terminated in these functional groups leaves MXenes high surface energy, as well as modifiability and re-manipulability of T_x. This also endows it with various required exceptional properties.

The performance of conventional noble metal electrode employed during the past often was limited by sluggish charge transfer kinetics. The produced toxic intermediates *via* oxidation process decreased activity of the immobilized enzyme [16]. Nevertheless, the dismissal of enzymes with distinctive selectivity will be associated with less reliable sensing signals in the applications of non-enzymatic glucose sensors, interfered by other endogenous substances [17]. 2D materials manifest the vital and intriguing material properties, such as large surface area, high surface to volume ratio, distinctive electronic structures and atomically thin layers [6]. Therefore, they have stolen the interest of a number of researchers. It is worth noting that 2D materials cannot be attained through conventional bulk structures [18]. Recent research efforts on 2D nanomaterials like graphene in applications have been further extended to wider perspectives [19]. However, some 2D materials that have been used to build sensitive sensing platforms are defective compared to MXenes. For example, the 2D material MoS_2 has hydrophobicity, low conductivity, and cannot be surface functionalized. The existence of impurities in carbon nanotubes leads to higher toxicity than other 2D family materials. It highly limited the application of biosensors, especially related sensing devices that must be attached to the human skin [20]. In addition, the applicable graphene-related polymers are problematic with shrinkage, swelling and folding or re-stacking of sheets. Also, their functionalization is limited by surface defects and edges [21]. Nevertheless, the metal-like conductivity, unique layered structure, excellent mechanical properties, and outstanding electrocatalytic performance of MXenes materials barge them to the forefront among similar 2D materials [22–28]. In addition, due to the existence of various complex interfering substances in real blood, high sensitivity and excellent selectivity are essential for glucose sensors. MXenes have a large specific surface area, large aspect ratio, excellent biocompatibility, good hydrophilicity and high electron transfer efficiency, which promises to satisfy the platform's demand for sensors. Additionally, the abundant surface functional groups of MXenes are capable to be modified for functionalization, which enables them to combine with other materials, especially lossy materials [29,30]. Finally it advantageously expands the extraordinary properties of MXenes, as well as adds synergistic effects for the construction of biosensors [31]. In summary, MXenes have demonstrated unprecedented potential for the usability of glucose biosensors. While some previous reviews have addressed this topic, it has not yet been presented in detail or surfaced. In this regard, we propose to provide a more specific and elaborated analysis of this crucial topic in order to advance this direction and to enlighten new researchers.

The primary objective of this review is to underscore the synthesis of MXenes materials and their advances in biosensors. We first summarize the related methods of etching and intercalation/layering during the synthesis of MXenes materials. Following this, with the data permit, we then discuss the main findings on synthesis procedure, structures, properties, and sensing mechanisms of glucose sensors made of composite materials involving MXenes. Subsequently, the promising prospects and challenges concerning MXenes-based glucose sensing technology are also discussed.

2. MXenes synthesis

The precursor of MXenes is MAX, a class of layered ternary carbides and nitrides [32], represented by the formula $M_{n+1}AX_n$ ($n = 1$, 2 or 3) [33,34]. The MAX phase has a unique crystal structure. It is formed by alternately stacking nearly close-packed M and A layers. And the M and X atomic layers in the MAX are interdigitated to form a compact hexagonal structure [35], where X atoms fill the octahedral void [36,37]. There is a a large ratio between M-X and M-A bond strengths. Because the M-A bond with the characteristics of hybrid covalent/metal/ionic bonds performed lower strength, compared to that of the M-X bond. Besides, it also contributes to the separate of MXenes from phase maximum. In general, it can be summarized that MXenes could be synthesized through bottom-up (components to MXenes films) [38] or top-down (MAX to MXenes) protocols [39]. Approximately, the first route refers to the operation starting from small molecules or atoms to crystal growth to further compose 2D materials, namely bottom-up methods. For example, chemical vapor deposition (CVD) [40], a fundamental method of this protocol, enables the preparation of MXenes, with excellent thermostability and no surface functional groups [41].

2.1. Direct HF etching

The top-down protocol, the second route, can be summarized as a wet chemical etching method, roughly divided into etching, delaminating, and intercalation [42]. Taking $Ti_3C_2T_x$, one of the most versatile and intriguing MXenes materials as examples, Fig. 1 has illustrated the synthesis pathway of few-layer MXenes.

Notably, diverse synthesis methods resulted in obtained MXenes with properties of different sizes, morphologies, functionalities, surface termination functional groups, *etc.* Therefore, it is crucial to adopt and tailor suitable synthetic methods to prepare MXenes to fit the requirements of investigations or particular applications [43,44]. Precursor MAX can be synthesized by mixing raw powders of M, A and X with a specific atomic ratio. Meanwhile, by pressuring less sintering or adjusting the heat and pressure, the growth direction of the crystal, denseness of the MAX material and the defined growth direction of the grains could be controlled. Meanwhile, it will consume large number of raw materials. The application of other methods is limited by the incapability to control grain growth direction. The classical approach is to generate MXenes with several incidental surface functional groups by selectively etching of M-A, whose bond energy is much lower than that of M-X, using a potent HF aqueous solution [11].

As Eq. S1 (Supporting information) showed, Naguib *et al.* [45] used this method to produce Ti_3C_2 multilayer nanosheets for the first time and systematically investigated the effects of etching time, temperature, particle size and M-A bond strength on 2D Ti_3C_2 production *via* the method involving HF. Then, HF selectively etched away the Al layer in MAX and replaced it [46,47]. While the

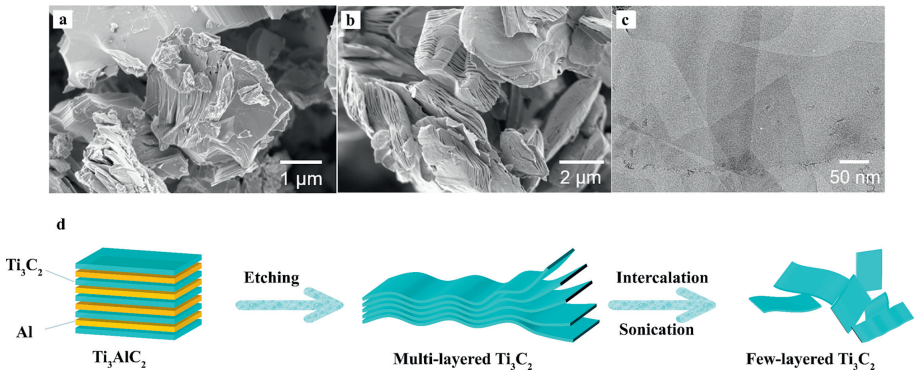

Fig. 1. (a) SEM micrograph of Ti_3AlC_2. (b) SEM micrograph of multi-layered Ti_3C_2. (c) TEM micrograph of few-layered Ti_3C_2. (a-c) Reprinted with permission [44]. Copyright 2021, Elsevier. (d) Schematic diagram of the synthesis pathway of few-layer MXenes. Reprinted with permission [43]. Copyright 2021, Elsevier.

Al layer was removed, more stable and stronger Ti-F bonds were deposited on the surface of MXenes. In the past decade, HF has been the most commonly used etchant for the synthesis of MXenes due to its relatively simplified operations, complete products synthesized with excellent controllability, *etc.* However, it is worth noting that the high toxicity, severe corrosivity and volatility of HF greatly raise the risk of related experiments [39]. Especially in the biological field, a minuscule amount of residual HF may lead to cell necrosis or even direct death of the organism [48]. Moreover, the method of HF etching MXenes results in lower yield and the products tends to generate more surface defects. Therefore, the exploration of eco-friendly and low-cost synthetic protocols for large-scale production of MXenes should be encouraged [49].

2.2. Enhanced methods for etching with F

Compared with the method of HF direct etching, the protocol of *in-situ* HF generation employs the reaction of fluoride with general-purpose inexpensive strong acid. It takes full advantage of the excellent selective corrosiveness of HF to Al and effectively avoids the hazards of direct HF application. Ghidiu *et al.* [50] developed a method for high-yield production of mostly monolayer MXenes flakes with large lateral dimensions and excellent quality. The method utilized a mixture of LiF and HCl to etch the precursor Ti_3AlC_2 powder and wash the resulting precipitate under heating at 40 °C for 45 h. Then the clay-like paste in wet conditions, formed flexible, free-standing films that simplified complex operations required for intercalation, layering and filtration techniques. Due to the intercalated H_2O and smaller size H^+ during the synthesis of MXenes, the interlayer space between MXenes is increased, which effectively weakens the interlayer interaction of MXenes nanosheets and reduces the self-stacking phenomenon of MXenes. In addition, other fluoride salts can also replace LiF such as tetrabutylammonium fluoride, CaF, NaF, KF, CsF [51]. As for HCl, it can be replaced by H_2SO_4. In addition to the *in-situ* generation of HF etching method, some other etching methods such as hydrothermal assisted method and molten salt method have been reported one after another.

To date, most MXenes preparation methods have been obtained by etching MAX whose A layer is Al, and protocols with Ti_3AlC_2 as the parent phase are particularly shared. Additionally, it will be possible rarely but well worth waiting that the investigations about the synthesis methods of MXenes by relying on the Al-free precursor MAX. Compared with the widely publicized Ti_3AlC_2, Ti_3SiC_2 is cheaper and popular in the market. Si element forms exceedingly strong Si-C bonds in MAX while some oxidants could effectively and selectively attack, then break the -C bonds. After the initial treatment with the oxidant, the silicon oxide can be dissolved using wet chemical etching by continuing to add HF. Based on this, Alhabeb *et al.* [52] tested various methods with oxidant-assisted (HF/HNO_3, $HF(/NH_4)_2S_2O_8$, $HF/KMnO_8$, HF/H_2O_2 and $HF/FeCl_3$) etching of silicon in Ti_3SiC_2 MAX and demonstrated that approach was a general method for preparing MXenes from Ti_3SiC_2MAX. Subsequently, the relevant chemical characterizations proved that the MXenes Ti_3C_2 prepared in the experiment had the same structure as the ones through the conventional method (obtaining the relevant MXenes film by exfoliation with an intermediate agent added).

2.3. Fluorine-free etching

Although the above methods avoid the direct use of HF, the preparation process involving F elements may still lead to environmental pollution as a result of the volatilization of HF. In addition, MXenes terminated with -F surface functional groups are less likely to be functionalized than those terminated with -OH and -O, thus limiting their wide application. Li *et al.* [53] developed a novel synthetic route for fluorine-free molten salts and successfully prepared MAX with Zn layer as the precursor of A phase and MXenes with surface terminated functional groups as Cl groups. In contrast to the conventional top-down approach, the Lewis acidity of the molten late metal halide $ZnCl_2$ results in a thermodynamic process that displaces Zn^{2+} from Al layers in the precursor MAX and replaces it by Zn atoms. After cleaning and exfoliating, termination of MXenes by Cl groups was achieved by further tailoring the ratio of $ZnCl_2$ and MAX (the A layers are Al element). Relevant experiments demonstrated augmented interlayer spacing of MXenes with Cl terminations instead of F-functionalized MXenes [54,55]. As such, the moderate molten salt environment and eco-friendly intermediate process without fluorine enable it an efficient synthetic route for the large-scale fabrication of MXenes.

Diluted HCl is milder and more stable than the conventional strong HF etchant. The employment of it will reduce the experimental risks and environmental pollution problems caused by HF due to strong corrosiveness, volatility and toxicity to a certain extent. The conventional HF direct etching method relies on the mechanism that the M-X bond performs much stronger than the M-A bond and the chemical activity of the A layer is higher. Thus, the M-A layer could be selectively etched and intercalated. This process essentially could be described as an electrochemical process involving charge transfer. Accordingly, Pang *et al.* [56] proposed a HF-free and facile route to synthesis MXenes. The fabrication of Ti_2AlC@CB/CFC composite electrodes was through carbon black (CB) additives and carbon fiber cloth (CFC) under appropriate mild heating conditions. And diluted hydrochloric acid was employed as an etchant. The overall E-etching reaction could be described as Eq. S2 (Supporting information) [54].

The CB/CFC composites were synthesized following a universal strategy based on thermal-assisted electrochemical etching approach [57]. The composites can form a 3D conductive network, which reduces the electrode ion diffusion resistance and promotes charge transfer. Meanwhile, the enhanced current density brought by appropriate heating conditions facilitates the dilute hydrochloric acid efficient etching.

In this context, Sun *et al.* [58] fabricated MXenes (Ti_2CT_x) for the first time using an electrochemical method with dilute hydrochloric acid as an etchant. Flash-dry silver paint and a copper wire were used to obtain the Ti_2AlC parallelepiped free-standing working electrode. Subsequently, the electrode was placed in an aqueous solution of HCl and the potential was tailored to initiate the electrochemical etching process.

The resulting washed Ti_2CT_x (MXenes) was terminated with -Cl, -O, and -OH groups, avoiding the detrimental effects of the -F group on functionalization of MXenes applications. As to obtain a core-shell product, the Ti layer in the MAX precursor could be further removed by increasing the potential during the etching process or the concentration of hydrochloric acid. The initial product was $Ti_2C(OH)_{2x}Cl_yO_z$, whose outer layer was composed of CDC with -Cl, -OH and -O surface functional groups) [55]. Under relatively fluorine-free environmental protection, it facilitated further extension of the range of products.

2.4. Choice of intercalation method

Multi-layered MXenes are the products synthesized by etching the precursor MAX [55]. The layering process is often managed to obtain single- or few-layered MXenes flakes with more intriguing properties and more versatility. Some articles refer to the multilayer MXenes for short, while the exfoliated ones are named d-MXenes.

Unlike graphene in the 2D material family, which is connected by weak van der Waals forces, M-X and M-A in MAX, are connected by metallic or covalent bonds [59]. This enhances the interlayer forces of m-MXenes (2–6 times that of monolithic graphite and graphene), resulting in suboptimal mechanical exfoliation alone (*e.g.*, scotch tape exfoliation and ultrasonic treatment). In addition, improper ultrasonic bath time control will result in MXenes excessively small flakes sizes and an increase in flaws [60].

Therefore, intercalators will contribute to structural enlargement and delamination. Because co-administration with intercalators will increase the interlayer spacing between MXenes including the c-lattice parameter, and effectively weaken the strong interaction between consecutive MXenes layers. Combined with other mechanical exfoliation methods, such as ultrasonic bath for delamination, d-MXenes with better properties and fewer defects can be obtained with high yield. Frequently-used intercalation materials include polar organic compounds [61] such as dimethyl sulfoxide [62], isopropylamine [63], tetrabutylammonium hydroxide [64], hydrazine [65] and choline [66], as well as partial cations such as Li^+, Na^+, K^+, $NH_4{}^+$, Sn^{4+} and Ca^{2+} in aqueous salt solutions.

Wu *et al.* [66] reported a water-free ionothermal synthesis approach for Ti_3C_2-MXene that was relatively non-hazardous. They employed the coexistence of choline chloride ($HOCH_2CH_2N(CH_3)_3Cl$) and oxalic acid-based deep eutectic solvents (DES). Then, the precursor Ti_3AlC_2 MAX was etched with NH_4F, then MXenes Ti_3C_2 was fabricated by ionothermal reaction at 100–180 °C. Notably, this set of experiments utilized choline cations to intercalate MAX, resulting in an enlarged interlayer spacing of 1.35 nm (larger than HF-Ti_3C_2 (0.98 nm)). Subsequently, the delamination of water bath sonication was implemented to fabricate MXenes.

The experiment above symbolizes the two-step approach: Selectively etch the A layers of the parent phase MAX with HF, *in-situ* generation of HF or other fluorine-free methods, and then add an intercalant to expand the interlayer spacing. Most of the synthesis methods of MXenes could be referred to these two steps carried out separately. However, in case the etching and intercalation of MAX would be completed simultaneously, this streamlined synthesis protocol will simplify the preparation process of single-layer or few-layer MXenes flakes to a certain extent, shorten the preparation time, increase the exfoliation rate and obtain products with fewer defects. Wu *et al.* [67] used HF and $Li^+/Na^+/Sn^{4+}$ to complete the etching process of MAX by one-step etching method. It is worth noting that based on the excellent specific capacity of Sn-based semiconductor materials, the interlayer spacing of Ti_3C_2-MXenes obtained by the one-step method is larger than that obtained by the conventional etch-and-insert method. In addition, Sn^{4+} could be uniformly distributed in the Ti_3C_2 MXenes matrix, so that HF and Sn^{4+} etching increases the c-lattice parameter of Ti_3C_2-MXenes from 18.5 Å to 24.84 Å [68].

3. Recent advances in MXenes-based glucose biosensor

This section focuses on the application of glucose sensors containing MXenes composites. The fabrication process, operation mechanism, relevant necessary parameters and merits of the sensor are systematically summarized. The relevant parameters of these developed sensors are listed in Table S1 (Supporting information).

3.1. Mechanism and applications of non-invasive glucose biosensors

Diabetes mellitus is a chronic disease characterized by a disorder of glucose regulation [1]. As one of the fastest growing diseases worldwide[2], about 693 million adults will suffer from the diabetes mellitus by 2045 as projected [69]. Diabetics are advised to measure their blood sugar levels several times a day [70]. However, the conventional method of finger sticking and using a dipstick meter has long afflicted diabetics with frequent finger pricks and accumulated pain from blood collections [3]. Non-invasive glucose sensing systems can effectively address this limitation and make diabetics suited for advanced diabetes care [4]. For more than two decades, people have been working on developing completely non-invasive electrochemical blood glucose monitoring sensors to enable more advanced blood glucose detection [5].

Sweat is capable of regulating body temperature and secreting a variety of biochemical components [71]. It is also an extremely intriguing biological fluid due to its non-invasive, continuous *in vitro* sampling point and ease of manipulation. Studies have demonstrated that the concentration of sweat, when properly collected, correlates reliably with concomitant blood sugar concentrations [6,7]. Fresh sweat samples, where glucose diffuses rapidly, can be easily collected on the surface of the skin for continuously monitoring glucose with appropriate methods. The synergistic and rapid development of materials science [1], electronic science and other fields contributes to smarter wearable sweat sensors meeting the requirements of non-invasive, real-time and continuous blood glucose monitoring [72]. They have been widely reported among the trends in personalized and preventive healthcare. Attribute to high sensitivity, strong anti-interference ability and long service life [71], they have created a brand-new platform to provide intermittent detailed information and parameters that can be unlikely attained *via* intermittent invasive blood sampling [73]. As the crucial elements of some wearable glucose sensor [71], 2D nanomaterials MXenes have aroused extensive attention owning to its extraordinary properties [74]. The high specific surface area stemmed from the unique layered structure of MXenes provide abundant surface active sites for the immobilization of enzymes related to

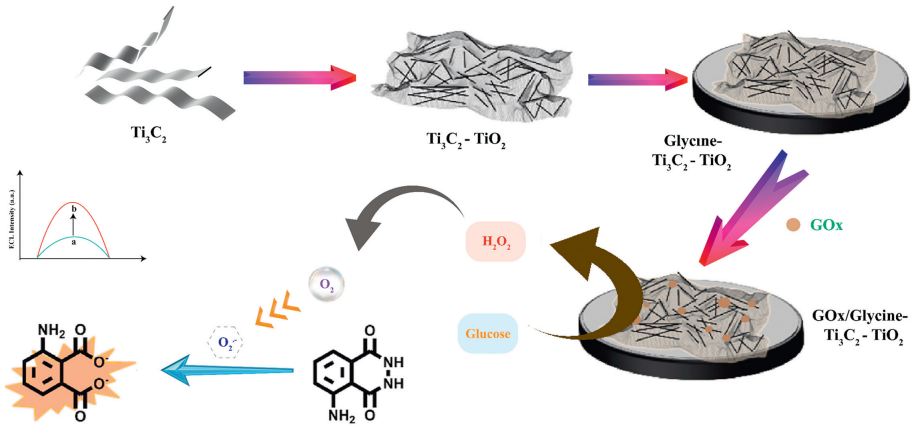

Fig. 2. Schematic diagram of manufacturing process of GOx/glycine-TiO_2-Ti_3C_2/GCE glucose electrochemiluminescence (ECL) bioluminescence sensor, and the amplification and generation of ECL signal. Reprinted with permission [75]. Copyright 2021, Wiley-VCH.

enzyme-based sensors. Meanwhile, its metallic electrical conductivity and outstanding point catalytic activity greatly enhance the sensitivity of wearable sensors. Moreover, excellent biocompatibility and hydrophilicity avoid skin irritation and tissue damage.

Sun *et al.* [75] developed a fast, reliable and linker-free electrochemiluminescence (ECL) biosensor based on Ti_3C_2 MXenes (TiO_2-Ti_3C_2) as the nanoplatform *in situ* growth of TiO_2 nanowires (limit of detection (LOD): 1.2 nmol/L, detection concentration range: 20 nmol/L-12 mmol/L). In a nitrogen atmosphere, KOH was added to the Ti_3C_2 solution prepared by etching Ti_3AlC_2 with a mixture of LiF and HCL to grow TiO_2 nanowires *in situ* on the surface by tailoring the reaction time of different samples. Besides, glycine-functionalized TiO_2-Ti_3C_2 was obtained with the addition of glycine after thorough cleaning. The polished glassy carbon electrode (GCE) and glycine-functionalized TiO_2-Ti_3C_2 were then used to fabricate activated electrodes and immersed in GOx solution for the immobilization on the electrodes. Subsequently, GOx/glycine-TiO_2-Ti_3C_2/GCE, glucose electrochemiluminescence (ECL) bioluminescence sensor was prepared successfully. The results indicate that the ECL intensity and stability of the TiO_2-Ti_3C_2 composite obtained under the condition of alkali oxidation for 3 h show the best performance. Hence, the *in-situ* growth of TiO_2 nanowires is available by tailoring the alkali oxidation time. Furthermore, relevant experiments demonstrates that TiO_2-Ti_3C_2 can oxidize H_2O_2 to generate O_2 and then reactes with it to generate $O_2^{\bullet-}$ reactive oxygen species. $O_2^{\bullet-}$ can oxidize luminol to 3-aminophthalate, enhancing the anode ECL emission of luminol, and generating the ECL signal. Fig. 2 illustrates schematically the structure and mechanism of developed biosensor. Attributed to metallic electrical conductivity and the large specific surface area of the TiO_2-Ti_3C_2 composite material, the electron transport distance is overwhelmingly shortened. Meanwhile, increased electron transport efficiency at the electrode interface leads to the signal amplification. At the same time, it is also beneficial to the immobilization of GOx on the electrode, attaining the dual effects of enhanced sensitivity and selectivity. In addition, the exposed Ti layer in the Ti_3C_2 layered structure can provide raw materials for the growth of TiO_2. The ECL nanoplatform has been employed for the detection of glucose in real samples such as human serum, fruit and sweat, and may provide strategies for real-time detection of blood glucose and early prevention of diabetes.

Oxidase produces its maximal effect only in a good oxygen-rich atmosphere, while the oxygen supply capacity of conventional wearable sweat biosensors is limited due to defects in manufacturing technology and structural design [76]. Moreover, in practical application, the sensing patch of the wearable sensor will suffer from friction and corrosion from the human skin. Therefore, restraint of enzymatic activity or denaturation and even inactivation seriously undermine the sensitivity and stability of the sensor. To our surprise, $Ti_3C_2T_x$ MXenes derived from 2D materials possess excellent biocompatibility, metallic conductivity and commendable electrocatalytic activity. Meanwhile, their unique 2D layered structure provides abundant surface active sites, which is beneficial to enhance the catalytic activity of enzymes and increase electron transport efficiency between it and the electrode [28]. Based on $Ti_3C_2T_x$ MXenes nanocomposites, Lei *et al.* [77] developed a multifunctional sweat biosensor with high selectivity and sensitivity for the detection of biomarkers in sweat. Fig. 3 describes the sensor integration system with sandwich structure. The porous fabric of the sweat absorbing layer below was employed to absorb sweat from the skin, which was then transmitted through a serpentine tunnel into the middle sensor layer. Several holes were excavated to facilitate the placement and replacement of diverse active sensors to meet the demands of different biomarker detections. In addition, the upper cover layer was left with obvious small holes to ensure that there were sufficient reactive oxygen flowing into the sensor. Fig. 3 depicts the oxygen-rich electrode of this sensor. In this experiment, CNTs were used to intercalate the $Ti_3C_2T_x$/PB (MXenes/Prussian blue) composite, and the intertwined CNTs and the intercalated $Ti_3C_2T_x$/PB layer formed a nest structure. It is worth noting that CNTs were not used alone, but mixed with $CaCO_3$ particles. When HCl is added to dissolve $CaCO_3$, it will lead to the formation of a porous ultrathin layered film, which is beneficial to oxygen transport. At the same time, the nested structure formed after intercalation and winding of CNTs had a larger specific surface area and more active sites, which facilitated the immobilization of enzymes. An oxygen-rich electrode with a solid-liquid-gas three-phase interface was fabricated after adding chitosan-embedded enzymes and back-sealing with flexible superhydrophobic carbon nanofiber membrane CFMs. Eventually, the detection sensitivity of glucose and lactate through chronoamperometry using artificial sweat are 35.3 μA mmol L^{-1} cm^{-2} and 11.4 μA mmol L^{-1} cm^{-2}, respectively. The detection limit of the glucose sensor and lactate sensor are 0.33×10^{-6} mol/L and 0.67×10^{-6} mol/L, respectively. In addition, experiments were designed to explore the selectivity and stability of the sensor. The experimental results indicates that there is no significant fluctuation of the current after the addition of interfering substances such as acetaminophen, acetylsalicylic acid, and uric acid. In contrast, the glucose sensor is exceedingly sensitive to the added glucose, proving the excellent selectivity of the developed biosensor. Moreover, the current fluctuation is ignorable within 15 days without addi-

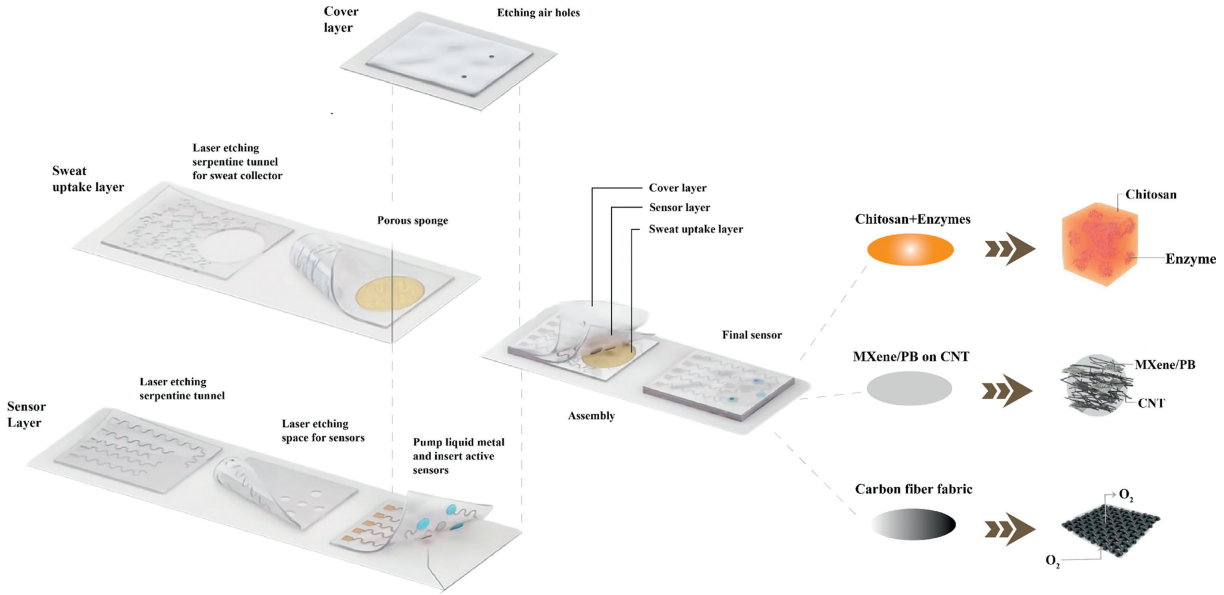

Fig. 3. The structure of the developed sensor patch system and schematic diagram of the oxygen-rich electrode of this sensor. Reprinted with permission [77]. Copyright 2019, Wiley-VCH.

tional calibrations for sensors, which reflects the stability of the prepared glucose sensor.

Tears are another ideal non-invasive biological fluid produced through the lacrimal gland to cover and protect the eye [78]. It is worth noting that the tear environment is purer than the blood environment. In addition, tear samples can be tested without preprocessing, which is capable to simplify operation to a certain extent. Simultaneously, relevant research [3] demonstrates that determination of concurrent are available through monitoring the concentrations of various metabolites in tears [79], making tears a prospective and significant substrate for non-invasively monitoring glucose levels [8].

Surface-enhanced Raman spectroscopy (SERS) is a potential trace analysis technique that has captured wide attention owning to its rapid detection, reliable sensitivity, low sample concentration and non-destructive properties [80]. However, fluorescence interference in the process of Raman detection is difficult to avoid, so it is crucial to find an active substrate with high stability, high sensitivity, and good reproducibility that can help reduce fluorescence interference. Regarded as one of the most versatile MXenes materials, $Ti_3C_2T_x$ are capable to attain the demand [80]. Notably, its unique 2D-layered structure leads to its excellent fluorescence quenching ability, huge specific surface area and negative charge on the surface. Therefore, $Ti_3C_2T_x$ can be used to load nanoparticles and adsorb the analytes to be studied. In addition, the excellent electrical conductivity and high catalytic activity make it an ideal material for enhanced SERS signals. Based on this, Cui *et al.* [81] loaded gold nanoparticles (AuNPs) onto the surface of MXenes to form a flexible surface-enhanced Raman scattering (SERS) substrate, aiming at non-invasive detection of blood glucose in tears (linear range was 1-50 μmol/L, the limit analyte concentration of detection was 0.32 μmol/L). First, the few-layer $Ti_3C_2T_x$ powder was obtained by HF etching and DMSO intercalation, and gold nanoparticles (AuNP) was prepared by the citrate reduction method. The paper/MXenes ($Ti_3C_2T_x$ loaded onto filter paper) was then dipped into the layered solution of AuNPs to deposit gold films to prepare flexible SERS substrates (named GMXeP). Fig. 4a shows the assembly and operation of this enzyme-based sensor, in which glucose oxidase (GOx) converts glucose into H_2O_2 and gluconic acid. Due to the unique peroxidase-like activity of AuNPs, H_2O_2 converts bright cabbage green (LMG) to malachite green (MG) to generate SERS signals. Experiments were also designed to demonstrate the excellent selectivity of the GMXeP substrate. Fig. 4b represents the SERS spectra of MG in artificial tears (whether glucose was added). Thus, it can be extrapolated that the two significantly distinct groups of signals have redundant Raman peaks. Fig. 4c manifests that at 10^{-5} mol/L R6G (Raman reporter molecules) concentration, the Raman signal is significantly enhanced after loading with AuNPs or applying (prepared by a specific method) GMXeP, respectively. In addition, the GMXeP group shows better Raman signal than the Paper/MXenes-AuNPs group due to the fluorescence quenching effect of MXenes. Moreover, with the artificial tear glucose control, the related experiments of the characterization of the relative standard deviation and Raman pattern are also verified due to the excellent selectivity, extraordinary sensitivity and reliable stability of the developed sensor.

3.2. Mechanism and applications of enzymatic glucose biosensors

Owning to the intrinsic properties of enzyme as the biological functional units, the enzyme-based biosensors for the detection of glucose have monopolize glucose sensing industry [81,82]. Nano-zinc oxide (ZnO) possesses various excellent physicochemical properties including enhanced surface-to-volume ratio, high electric point, high electron transport capability and biocompatibility. However, its application in electrochemistry have been limited by its high resistivity [83–85]. Combining ZnO with MXenes which manifests excellent electrical conductivity is expected to enhance the performance of the electrochemical sensors. Accordingly, Myndrul *et al.* [86] prepared a stretchable enzyme electrochemical glucose sensor based on ZnO-TPs/MXenes nanocomposites, which exhibited enhanced sensitivity (29 μA mmol L^{-1} cm^{-2}), low limit of detection (LOD ≈ 17 μmol/L) for human sweat analysis and a broad linear detection range (LDR = 0.05-0.7 mmol/L). The prepared ZnO TPs/MXenes/GOx electrodes also exhibites up to 30% mechanical stability. Firstly, ZnO-TPs-ZnO tetrapods (ZnO-TPs) were prepared by catalyst-free oxidation metal vapor transport method. And MXenes Ti_3C_2 was synthesized by HCL-LiF mixed etching of Ti_3AlC_2 (MAX) with the intercalation and layering of Li^+. The pulverized MXenes nanosheet-decorated ATPES solution-functionalized ZnO TPs were then coated with an additional layer of Nafion polymer (5 μL of 2% ethanol solution neutralized to pH

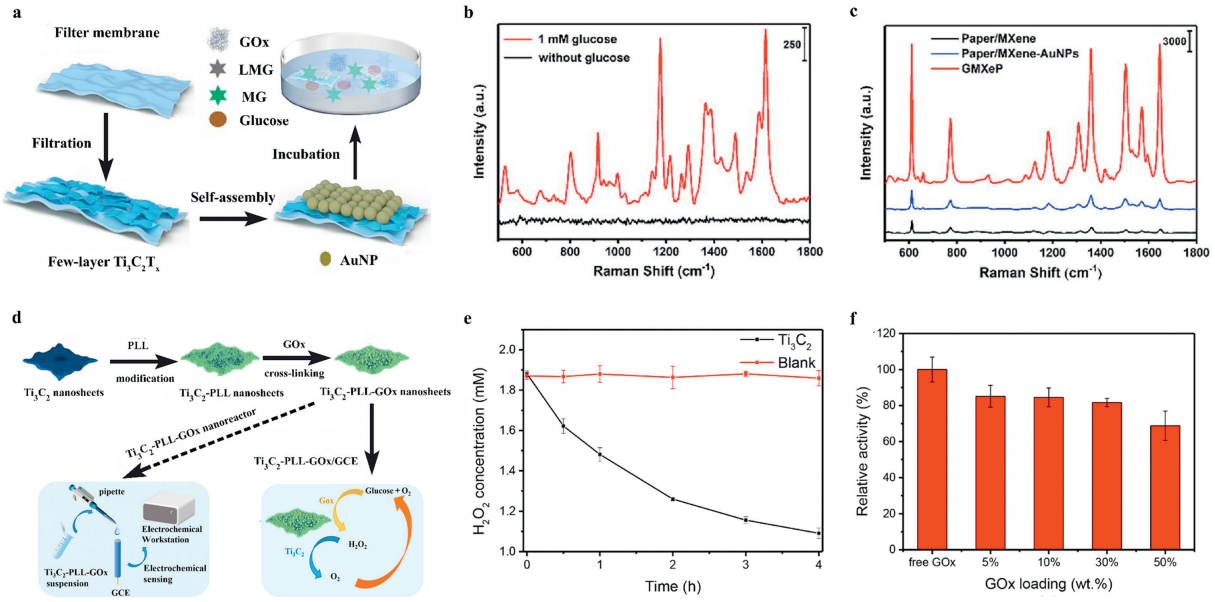

Fig. 4. (a) Schematic illustration of the synthetic route of GMXeP. (b) The SERS spectra of MG in artificial tears in two circumstances. (c) SERS spectra of R6G attained *via* divergent substrates. (a-c) Reprinted with permission [81]. Copyright 2019, Wiley-VCH. (d) Schematic illustration of the synthetic route of Ti_3C_2-PLL-GOx nanosheets, details of mechanism of reaction with glucose and its employment in the application of obtaining electrochemical sensing platform. (e) Line chart of the decomposition with the catalysis of Ti_3C_2-PLL-GOx and reference substance. (f) Histogram of relative activity attained under the different circumstances of diverse GOx loading (5, 10, 30, and 50 wt%). (d-f) Reprinted with permission [43]. Copyright 2021, Wiley-VCH.

7) to coat the skin-attachable and stretchable sensors. The active surface of tetrapod-like ZnO (ZnO TPs) enhances the efficiency of detection performance. In addition, the decoration of MXenes nanosheets with high electron transport efficiency increase the catalytic activity of the developed nanocomposites [85]. Subsequently, the electron transfer constants were calculated by the slopes of the linear parts of the Laveron curves of different electrodes. Therefore, conclusion demonstrated that the MXenes-modified ZnO-TP had higher electron transport efficiency. In addition, the concentration of free oxygen around the electrode determines the strength of the reduction current, with the conversion of FAD influencing the concentration of free oxygen.

The prosthetic group (FAD of GOx of aerobic dehydrogenases) participates in the reaction of glucose and consumes oxygen, converting it into its own prototype -$FADH_2$, which is then oxidized back to FAD and generates protons to reduce water molecules to H_2O_2. Related equation could be found in Eq. S3 (Supporting information). Subsequently, selectivity tests manifestes that the ZnO TP/MXenes/GOx-based electrode still has high selectivity for glucose only after adding various interfering substances.

A glucose sensor with excellent stability, repeatability and reproducibility was developed based on Au/MXenes nanocomposites to fabricate GOx/Au/MXenes/Nafion/GCE biosensor electrodes (sensitivity of 4.2 μA mmol L^{-1} cm^{-2}, a wide linear range from 0.1 mmol/L to 18 mmol/L and a lower detection limit of 5.9 μmol/L) [87]. To begin with, MXenes were prepared by selectively etching Ti_3AlC_2 parent phase with HF. Then the gold nanocrystalline Au clusters modified MXenes and the negatively charged polyelectrolyte matrix Nafion were employed to immobilize GOx and perform solubilization, respectively. Eventually, the developed glucose biosensor was obtained on GCE. The prosthetic group FAD of GOx of aerobic dehydrogenases participates in the reaction of glucose and consumes oxygen to convert to its reduced $FADH_2$, which is subsequently oxidized back to FAD and generates protons to reduce water molecules to H_2O_2. In addition, the concentration of glucose could be determined by monitoring the concentration of H_2O_2 [88]. Related equations could be found in Eqs. S3 and S4 (Supporting information).

The direct electron transfer (DET) efficiency between enzymes and electrodes determines the sensitivity, selectivity and many other paramount sensing properties of enzyme-based glucose biosensors [89–93]. Since the redox active center of the protein is embedded in the outer shell of the protein [1], it is vital to attain DET between the protein and the electrode surface by other methods. Researchers proposed to use conductive nanomaterials to promote DET [2]. Therefore, Au nanoparticles based on the nanomaterial MXenes were used to improve the insulating effect of the protein shell on direct electron transfer as well as provide appropriate microenvironment to maintain normal enzyme activity. Moreover, it is worth noting that the excellent conductivity and high specific surface area of MXenes promote the electron transfer between the enzyme (GOx) active redox center and GCE. The TEM analysis of the microstructure of Au/MXenes nanocomposites requires ultrasonic treatment to separate the individual MXenes sheet. However, most of the Au nanoparticles are still almost uniformly distributed on the surface of the exfoliated ultra-thin MXenes nanosheets superior. This demonstrates the strong interaction between Au nanoparticles and MXenes nanosheets.

Similar to the previous experiment, another research utilizes MXenes to overcome the inadequate electron transport defect between GOx and bare glassy carbon electrodes owning to the encapsulated protein layers [94]. In the experiment, the direct etching method of HF was used and tetrabutylammonium hydroxide (TBAOH) was employed as the intercalating agent to expand the interlayer spacing of MXenes. Subsequently, the layered MXenes were obtained after ultrasonic treatment. Subsequently, Ti_3C_2-HF/TBA/GOx was obtained by modifying the glassy carbon electrode with layered MXenes and simultaneously supporting GOx as a substrate. The practicality and feasibility of the sensing platform are also demonstrated by testing the developed sensor with real human serum and daily food. The heterogeneous electron-transfer (HET) capability of Ti_3C_2-HF/TBA was measured by cyclic voltammetry (CV) compared to the precursor MAX and MXenes without TBAOH intercalation. It indicates that the huge specific surface area of the layered MXenes provides abundant attachment

sites for the loading of a large number of enzymes. The smaller size of the delamination leads to the reduction of the distance between the enzyme and the electrode. Therefore, the closer distance and the metal-like conductivity of MXenes enhances the electron transport efficiency. Interfering substances such as uric acid and L-ascorbic acid were added to induce signal of the sensing platform. Also, the performance was valuated with real human serum and daily beverages. The results demonstrate the practicality, feasibility and reliable selectivity of the proposed sensing platform.

A toxic intermediate (H_2O_2) produced during the oxidation of glucose by GOx usually inhibits the activity of Gox [95]. To address this issue, a strategy was proposed. By constructing a cascade reaction system, intermediate by-product H_2O_2 would be induced to decomposite [96]. However, in practical situations, the application of enzymes will involve many issues, such as conditions of use, which complicates the operation. Studies have shown that Ti_3C_2 MXenes has the ability to catalyze the decomposition reaction of H_2O_2 [97]. Simultaneously, Ti_3C_2 MXenes can also be used as a matrix for immobilizing GOx. Accordingly, Wu *et al.* [43] developed a 2D cascade nanoreactor based on Ti_3C_2-PLL-GOx nanocomposites for glucose detection (detection limit of 2.6 μmol/L, detection sensitivity of 38.18 μA mmol L^{-1} cm^{-2}).

Specifically, add 1-(3-dimethylaminopropyl)-3-ethylcarbodiimide hydro (EDC) and GOx (to promote the binding of the carboxyl group in GOx to the amino group in the PLL chain) to the Ti_3C_2-PLL collected by centrifugation after mixing PLL (polylysine) and Ti_3C_2. Then, alumina powder polished GCE was deposited with Ti_3C_2-PLL-GOx suspension. Subsequently, Ti_3C_2-PLL-GOx/GCE electrode was obtained after natural drying. The large specific surface area of Ti_3C_2 provides a huge adsorption surface for the loading of GOx, and it have been experimentally proved to have a faster loading speed and larger adsorption capacity (about 5 times) than bimodal mesoporous silica (BMS) microspheres. In addition, the metal-like conductivity of MXenes nanomaterials effectively promotes the DET between the protein and the electrode surface, improving the electron transport efficiency of the developed electrode and thus the detection sensitivity. According to the designed equivalent circuit, the resistance of Ti_3C_2 modified GCE is only 2.26 Ω, which was much smaller than the resistance of bare GCE electrode (70.82 Ω).

Under the catalysis of the excellent electrical conductivity of Ti_3C_2 nanosheets, oxygen is generated by the decomposition of H_2O_2. It could be reused for the glucose oxidation reaction, thereby increasing the reaction rate of glucose oxidation. Meanwhile, the use of highly conductive Ti_3C_2 substrate to immobilize the enzyme is beneficial to accelerate the electron transport speed in the glucose biosensor, thereby improving the detection sensitivity. In addition, due to the huge specific surface area of MXenes, the active sites of the immobilized GOx are fully exposed to the external environment, facilitating the enzymatic reaction. Fig. 4d has demonstrated details of mechanism of reaction with glucose and its employment in the application of obtaining electrochemical sensing platform.

Also, designed experiments verifies the catalytic properties of MXenes Ti_3C_2 for the decomposition of H_2O_2. From Fig. 4e, it could be concluded that the amount of H_2O_2 decomposed in the system is about 0.79 mmol/L in 4 h. This indicates that MXenes Ti_3C_2 are capable to catalyze the decomposition of H_2O_2.

The enzymatic activity of Ti_3C_2-PLL-GOx nanosheets were carefully probed by designed experiments. As shown in Fig. 4f, owning to the high loading of GOx, the tight structure between GOx molecules reduces the electrode activity, which affects the application of active sites. Moreover, the relative activities of Ti_3C_2-PLL-GOx nanosheets with GOx loadings of 5% and 10% are the best.

3.3. Mechanism and applications of non-enzymatic glucose biosensors for the detection of glucose

Although the enzyme has high specificity and catalytic efficiency for its substrate, this fragile biomolecule needs a relatively strict physiological environment to perform its function. For example, GOx has been commercialized due to its relatively stability in comparison to other enzymes within the same group. However, the immobilization process of enzyme on substrate requires cumbersome and complex operations [98,99]. Moreover, the high temperature sensitivity of biomolecules limits its further application in fermentation processes [100,101]. GOx has been demonstrated to be denatured and inactivated when the ambient temperature exceeds 40 °C. Also, the activity of GOx is affected by the alteration and volatility of the actual relative humidity, oxygen concentration [102] and pH value [4]. Relevant experiments [100] have indicated that GOx will undergo irreversible denaturation at pH $<$ 2 or pH $>$ 8. It is worth noting that owning to the inherent and intrinsic fragility of biomolecules, GOx-based sensors are almost incapable of resisting any chemical deformations and thermal environment. However, the production process of GOx inevitably involves the process of comprehensive disinfection and sterilization, which would set barriers for the application, transport and storage of enzyme-based sensors [103]. Undoubtedly, successfully mass-produced enzyme-based sensors have dominated the glucose sensing market. But the proposal of freeing glucose sensors from the dependence on biological functional units still motivates researchers to develop more reliable, stable and practical non-enzymatic sensing platform [104,105]. NiCo-LDH is the abbreviation of nickel-cobalt layered double hydroxides. This layered double hydroxides (LDHs) $\{[M_{1-x}^{2+}M_x^{3+}(OH)_2]^{x+}[A_{x/n}^{n-}]^{x-} \cdot mH_2O\}$ possess outstanding specific surface area, favourable electrical conductivity and catalytic activity after being doped with Co and Ni. 2D materials (MXenes) are characteristic of metal-like conductivity, high electron transport efficiency and high specific surface area. The 3D composites formed by further depositing NiCo-LDH on MXenes with metal-like conductivity, high electron transport efficiency and high specific surface area are expected to be used in sensor research. Accordingly, Li *et al.* [106] developed a glucose biosensor with a wide linear range (0.002-4.096 mmol/L), low LOD (0.53 mmol/L) and fast response function (3s) based on 3D porous MXenes/NiCo-LDH nanocomposites. In the beginning, the multi-layer Ti_3C_2 obtained by etching the Ti_3AlC_2 parent phase with HF solution was subjected to exfoliation operation to obtain single or few layer Ti_3C_2 nanosheets. Subsequently, NiCo-LDH-MXenes was prepared by hydrothermal method. And then it was deposited on the top of GCE to obtain the developed sensor. In the hydrothermal reaction, the hydroxyl groups were generated by the redox reaction of methanol and nitrate [107]. Then they reacted with Ni^{2+} and Co^{2+} to form monomers on the negatively charged MXenes nanoplatform [108,109]. Subsequently, the primary particles formed by the combination of these hydroxide monomers were deposited on the surface of MXenes to complete the preparation of the 3D composite. The demands of proton reduction of Ni/Co(III) to Ni/Co(II) guided the deprotonation of glucose in alkaline environment.

The glucose oxidation reaction process on the obtained electrode surface could be extrapolated as Eq. S5 (Supporting information). To be mentioned, the developed 3D porous composites are capable to convert the diffusions from planar to thin layer. Also, more channels will be provided for electrolyte diffusion and sufficient contact with the active material. Additionally, the obtained composites performed positive catalytic activity due to MXenes excellent electrical conductivity, high electron transport efficiency and hydrophilicity. According to the measurement *via* CV, the anode peak current of MXenes/NiCo-LDH (90.82 μA) is apparently

higher than NiCo-LDH (35.82 μA). Moreover, the addition of many other interfering substances (fructose, ascorbic acid, dopamine *etc.* at 0.1 mmol/L) doesnot have a significant effect on the current of the MXenes/NiCo-LDH/GCE electrode. And the electrode current is extremely sensitive to 0.5 mmol/L glucose, which reflectes the developed sensor reliable selectivity. In addition, the excellent reproducibility, reliable stability and practicability of the MXenes/NiCo-LDH/GCE electrode are verified by analyzing real blood samples and measuring the current response (0.1 mol/L KOH solution added with 1 mmol/L glucose at different time periods).

4. Conclusion and outlook

This review mainly focuses on the main synthetic route of MXenes, as well as the state-of-the-art recent advances of biosensors involving MXenes as an electrode modifier for glucose detection. Some details including the preparation scheme, performance and sensing mechanism are also discussed.

Accordingly, in the domain of biosensing, it is undoubtedly that composites involving unique two-dimensional layered nanomaterials MXenes with extraordinary properties have become a research hotspot [71]. Substrates for biosensing are projected to possess excellent biocompatibility and hydrophilicity to shun tissue damage and rejection. The construction of a reliable detection platform requires favourable conductive sensing materials for the effective enhancement of the electron transport efficiency and glucose oxidation kinetics [17]. Meanwhile, attributed to the remarkable synergistic effect, the fabrication of polymer modified composites is highly expected to employ suitable substrates. Those with a sufficiently large specific surface area could provide abundant active sites and support other materials such as metal particles [110,111].

However, it is worth noting that most of the related researches concentrate on the approaches to enhance the sensing performance of glucose sensors, such as minimum detection limit and linear range. However, the fact is that the fabrication of MXenes-based sensing materials for these glucose sensing platforms is relatively complicated and costly [112]. Besides, the synthesis protocols involved with HF may produce MXenes terminated with -F surface functional groups (more unlikely to be functionalized) and still are problematic with the environmental pollution as well as the augmented experimental operation risk. Furthermore, improper time control of ultrasonic bath will give rise to too small size of MXenes flakes and more defects [113]. Consequently, enhanced synthesis process should be encouraged to develop a new path for the commercialization and large-scale production of polymer modified composites.

Continuous exploration to revolutionize in future sensors will be urged in the development tendency of miniaturized biosensing devices with outstanding sensing performance. Thus, fascinating multifunctional characteristic of nanomaterials MXenes push them into practical applications and draw a blueprint for the development of miniature glucose sensors. With rational and ingenious design, this miniature sensor is capable to be implanted subcutaneously. By being attached to or into blood vessel walls, it makes completely real-time, non-invasive blood level detection available. Afterwards, this portable microsensor with continuous detection capability can provide a perfect physiological environment for enzyme-based sensors after being implanted in the human body. It may be the best method to remedy the inherent limitation (arduous to provide the harsh environmental conditions for external-applied enzyme-based sensors). MXenes for such portable, implantable biosensors universally contact with human skin or other tissues directly.

As a nanocomposite material that has only emerged in the last decade, MXenes for such portable, implantable biosensors universally contact with human skin or other tissues directly. Despite their application prospect for therapeutics created by their tremendous properties, challenges still exist unless MXenes are demonstrated as biomedical purposes-satisfied. Therefore, their cytotoxicity, biodegradability and biocompatibility for in-*vivo* clinical translation need to be further investigated to prevent biofouling [76].

Declaration of competing interest

The authors declare that they have no known competing financial interests or personal relationships that could have appeared to influence the work reported in this paper.

Acknowledgment

Fanghua Li acknowledges the funding support from Harbin Institute of Technology, China (No. FRFCU5710053121).

Supplementary materials

Supplementary material associated with this article can be found, in the online version, at doi:10.1016/j.cclet.2023.108241.

References

[1] D. Wang, G. Xu, X. Zhang, et al., Sens. Actuators B: Chem. 359 (2022) 131512.
[2] H. Sun, P. Saeedi, S. Karuranga, et al., Diabetes Res. Clin. Pr. 183 (2022) 109119.
[3] W. Wu, L. Lin, Z. Lin, et al., Obes. Surg. 28 (2018) 3087–3094.
[4] D.W. Hwang, S. Lee, M. Seo, T.D. Chung, Anal. Chim. Acta. 1033 (2018) 1–34.
[5] J. Zhu, E. Ha, G. Zhao, et al., Coord. Chem. Rev. 352 (2017) 306–327.
[6] Z. Juan, M. Dong, X. Zhang, Chin. J. Anal. Chem. 50 (2021) 87–96.
[7] Y.T. Liu, P. Zhang, N. Sun, et al., Adv. Mater. 30 (2018) e1707334.
[8] U. Yorulmaz, A. Özden, N.K. Perkgöz, F. Ay, C. Sevik, Nanotechnology 27 (2016) 335702.
[9] S.H. Talib, Z. Lu, B. Bashir, et al., Chin. Chem. Lett. 34 (2022) 2213–2762.
[10] M. Naguib, M. Kurtoglu, V. Presser, et al., Adv. Mater. 23 (2011) 4248–4253.
[11] Z. Bao, C. Lu, X. Cao, et al., Chin. Chem. Lett. 32 (2021) 2648–2658.
[12] Y. An, Y. Tian, J. Feng, Y. Qian, Mater. Today 57 (2022) 146–179.
[13] B. Lu, Z. Zhu, B. Ma, et al., Small 17 (2021) 2100946.
[14] Y. Wang, W. Feng, Y. Chen, Chin. Chem. Lett. 31 (2020) 937–946.
[15] M. Naguib, Y. Gogotsi, Acc. Chem. Res. 48 (2015) 128–135.
[16] H.C. Wang, A.R. Lee, J. Food Drug Anal. 23 (2015) 191–200.
[17] R. Reghunath, K. devi, K.K. Singh, Nano-Struct. Nano-Objects. 26 (2021) 100750.
[18] M. Burt, G. Roberts, N. Aguilar-Loza, S. Stranks, Diabetes Technol. Ther. 15 (2013) 241–245.
[19] R.A. Soomro, S. Jawaid, Q. Zhu, Z. Abbas, B. Xu, Chin. Chem. Lett. 31 (2020) 922–930.
[20] P.K. Kalambate, N.S. Gadhari, X. Li, et al., Trends Anal. Chem. 20 (2019) 115643.
[21] A.T. Lawal, Biosens. Bioelectron. 141 (2019) 111384.
[22] A. Sanati, Y. Esmaeili, E. Bidram, et al., Appl. Mater. Today 26 (2022) 101350.
[23] I. Lee, D. Probst, D. Klonoff, K. Sode, Biosens. Bioelectron. 181 (2021) 113054.
[24] M.J. Tierney, J.A. Tamada, R.O. Potts, L. Jovanovic, S. Garg, Biosens. Bioelectron. 16 (2001) 621–629.
[25] D. Zhang, S. Yang, X. Fang, et al., Chin. Chem. Lett. 33 (2022) 4669–4674.
[26] M. Xu, P. Zhao, C.Y. Tang, X. Yi, X. Wang, Chin. Chem. Lett. 33 (2022) 3818–3822.
[27] B. Guan, X. Sun, Y. Zhang, et al., Chin. Chem. Lett. 32 (2021) 2249–2253.
[28] W. Yuan, X. Qu, Y. Lu, et al., Chin. Chem. Lett. 32 (2021) 2021–2026.
[29] S.K. Bhardwaj, H. Singh, M. Khatri, K.H. Kim, N. Bhardwaj, Biosens. Bioelectron. 202 (2022) 113995.
[30] B. Xu, Y. Gogotsi, Chin. Chem. Lett. 31 (2020) 919–921.
[31] S. Alwarappan, N. Nesakumar, D. Sun, T.Y. Hu, C.Z. Li, Biosens. Bioelectron. 205 (2022) 113943.
[32] M.M. Baig, I.H. Gul, S.M. Baig, F. Shahzad, J. Electroanal. Chem. 904 (2022) 115920.
[33] W. Jiang, X. Zou, H. Du, et al., Chem. Mater. 30 (2018) 2687–2693.
[34] C. Li, X. Zhang, K. Wang, X. Sun, Y. Ma, Chin. Chem. Lett. 31 (2020) 1009–1013.
[35] X. Xu, L. Yang, W. Zheng, et al., Mater. Today Energy 2 (2022) 100080.
[36] Z.M. Sun, Int. Mater. Rev. 56 (2011) 143–166.
[37] M. Barsoum, Introduction History of the MAX Phases References, MAX Phases: M. Barsoum, Properties of Machinable Ternary Carbides and Nitrides, Wiley-VCH Verlag GmbH & Co. KGaA, Weinheim, 2013, pp. 1–12.
[38] M. Baig, I. Gul, S. Baig, F. Shahzad, J. Electroanal. Chem. 904 (2021) 115920.
[39] A. Zamhuri, G.P. Lim, N.L. Ma, K.S. Tee, C.F. Soon, Biomed. Eng. Online 20 (2021) 33.
[40] C. Xu, L. Wang, Z. Liu, et al., Nat. Mater. 14 (2015) 1135–1141.
[41] D. Dhamodharan, V. Dhinakaran, H.S. Byun, Carbon 192 (2022) 366–383.
[42] Y. Yao, J. Zhao, X. Yang, C. Chai, Chin. Chem. Lett. 32 (2021) 620–634.

[43] M. Wu, Q. Zhang, Y. Fang, et al., J. Colloid Interface Sci. 586 (2021) 20–29.
[44] L. Verger, C. Xu, V. Natu, et al., Curr. Opin. Solid State Mater. Sci. 23 (2019) 149–163.
[45] M. Naguib, M. Barsoum, Y. Gogotsi, et al., Adv. Mater. 33 (2021) 2103393.
[46] S.B. Ambade, R.B. Ambade, W. Eom, et al., Adv. Mater. Interfaces 5 (2018) 1801361.
[47] C. Zhou, X. Zhao, Y. Xiong, et al., Eur. Polym. J. 167 (2022) 111063.
[48] H. Hu, S. Wei, S. Lin, L. Chen, C. Pan, Asian J. Surg. 341 (2022) 111468.
[49] X. Li, Y. Lu, Q. Liu, Talanta 235 (2021) 122726.
[50] M. Ghidiu, M.R. Lukatskaya, M.Q. Zhao, Y. Gogotsi, M.W. Barsoum, Nature 516 (2014) 78–81.
[51] L. Li, J. Wen, X. Zhang, ChemSusChem 13 (2020) 1296–1329.
[52] M. Alhabeb, K. Maleski, T. Mathis, et al., Angew. Chem. Int. Ed. 57 (2019) 5444–5448.
[53] M. Li, J. Lu, K. Luo, et al., J. Am. Chem. Soc. 141 (2019) 4730–4737.
[54] W. Sun, S.A. Shah, Y. Chen, et al., J. Mater. Chem. A 5 (2017) 21663–21668.
[55] S. Kajiyama, L. Szabova, H. Iinuma, et al., Adv. Energy Mater. 7 (2017) 1601873.
[56] S. Yang, P. Zhang, F. Wang, et al., Angew. Chem. Int. Ed. 57 (2018) 15491–15495.
[57] S.Y. Pang, Y.T. Wong, S. Yuan, et al., J. Am. Chem. Soc. 141 (2019) 9610–9616.
[58] W. Sun, S. Shah, Y. Chen, et al., J. Mater. Chem. A 5 (2017) 103360475.
[59] S. Wu, H. Wang, L. Li, et al., Chin. Chem. Lett. 31 (2020) 961–968.
[60] M. Malaki, A. Maleki, R.S. Varma, J. Mater. Chem. A 7 (2019) 10843–10857.
[61] M. Jeon, B.M. Jun, S. Kim, et al., Chemosphere 261 (2020) 127781.
[62] G. Lv, J. Wang, Z. Shi, L. Fan, Mater. Lett. 219 (2018) 45–50.
[63] X. Li, F. Ran, F. Yang, J. Long, L. Shao, Trans. Tianjin Univ. 27 (2021) 217–247.
[64] M. Naguib, R.R. Unocic, B.L. Armstrong, J. Nanda, Dalton Trans. 44 (2015) 9353–9358.
[65] M.R. Lukatskaya, O. Mashtalir, C.E. Ren, et al., Science 341 (2013) 1502–1505.
[66] J. Wu, Y. Wang, Y. Zhang, et al., J. Energy Chem. 47 (2020) 203–209.
[67] A. Hu, J. Yu, H. Zhao, H. Zhang, W. Li, Appl. Surf. Sci. 505 (2020) 144538.
[68] A.Y. Hu, J.L. Yu, H. Zhao, H. Zhang, W. Li, Appl. Surf. Sci. 505 (2020) 144538.
[69] D.W. Bowden, Curr. Diab. Rep. 2 (2002) 191–200.
[70] K. Berg, Physcian Sportsmed. 7 (1979) 71–79.
[71] G. Li, D. Wen, Chin. Chem. Lett. 32 (2021) 221–228.
[72] J. Zhou, D. Men, X.E. Zhang, Chin. J. Anal. Chem. 50 (2022) 87–96.
[73] Q. Chen, Y. Zhao, Y. Liu, Chin. Chem. Lett. 32 (2021) 3705–3717.
[74] H. Riazi, G. Taghizadeh, M. Soroush, ACS Omega 6 (2021) 11103–11112.
[75] Y. Sun, P. Li, Y. Zhu, et al., Biosens. Bioelectron. 194 (2021) 113600.
[76] M. Mathew, C.S. Rout, Curr. Opin. Electrochem. 30 (2021) 100782.
[77] Y. Lei, W. Zhao, Y. Zhang, et al., Small 15 (2019) 1901190.
[78] J.A. Clayton, N. Engl. J. Med. 378 (2018) 2212–2223.
[79] J.R. Sempionatto, L.C. Brazaca, L. García-Carmona, et al., Biosens. Bioelectron. 137 (2019) 161–170.
[80] Q. Huang, J. Li, Mater. Lett. 204 (2017) 85–88.
[81] X. Cui, J. Li, Y. Li, et al., Spectrochim. Acta A 266 (2022) 120432.
[82] T. Unmüssig, A. Weltin, S. Urban, et al., J. Electroanal. Chem. 816 (2018) 215–222.
[83] V. Myndrul, L. Vysloužilová, A. Klápšťová, et al., Coatings 10 (2020) 1199.
[84] M. Pavlenko, V. Myndrul, G. Gottardi, et al., Materials 13 (2020) 1987.
[85] A. Tereshchenko, M. Bechelany, R. Viter, et al., Sens. Actuators B: Chem. 229 (2016) 664–677.
[86] V. Myndrul, E. Coy, N. Babayevska, et al., Biosens. Bioelectron. 207 (2022) 114141.
[87] R.B. Rakhi, P. Nayak, C. Xia, H.N. Alshareef, Sci. Rep. 6 (2016) 36422.
[88] F. Zhang, Q. Wan, C.X. Li, et al., Chin. J. Chem. 21 (2010) 1619–1623.
[89] J. Wang, Chem. Rev. 108 (2008) 814–825.
[90] X. Kang, J. Wang, H. Wu, et al., Biosens. Bioelectron. 25 (2009) 901–905.
[91] B. Unnikrishnan, S. Palanisamy, S.M. Chen, Biosens. Bioelectron. 39 (2013) 70–75.
[92] H. Liu, C. Duan, C. Yang, et al., Sens. Actuators B: Chem. 218 (2015) 60–66.
[93] S. Deng, G. Jian, J. Lei, Z. Hu, H. Ju, Biosens. Bioelectron. 25 (2009) 373–377.
[94] H.L. Chia, C.C. Mayorga-Martinez, N. Antonatos, et al., Anal. Chem. 92 (2020) 2452–2459.
[95] Z. Gu, A.A. Aimetti, Q. Wang, et al., ACS Nano 7 (2013) 4194–4201.
[96] X. Liu, Y. Liu, J. Wang, T. Wei, Z. Dai, ACS Appl. Mater. Interfaces 11 (2019) 23065–23071.
[97] L. Lorencova, T. Bertok, E. Dosekova, et al., Electrochim. Acta 235 (2017) 471–479.
[98] M. Wei, Y. Qiao, H. Zhao, et al., Chem. Commun. 56 (2020) 14553–14569.
[99] S. Fu, G. Fan, L. Yang, F. Li, Electrochim. Acta 152 (2015) 146–154.
[100] R. Wilson, A.P.F. Turner, Biosens. Bioelectron. 7 (1992) 165–185.
[101] E. Shoji, M.S. Freund, J. Am. Chem. Soc. 123 (2001) 3383–3384.
[102] J.A. Bauer, M. Zámocká, J. Majtán, V. Bauerová-Hlinková, Biomolecules 12 (2022) 12030472.
[103] Q. Dong, H. Ryu, Y. Lei, Electrochim. Acta 370 (2021) 137744.
[104] S. Park, H. Boo, T.D. Chung, Anal. Chim. Acta 556 (2006) 46–57.
[105] I.U. Hassan, H. Salim, G.A. Naikoo, et al., J. Saudi Chem. Soc. 25 (2021) 101228.
[106] M. Li, L. Fang, H. Zhou, et al., Appl. Surf. Sci. 495 (2019) 143554.
[107] A. Sinha, Dhanjai, H. Zhao, et al., Trends Anal. Chem. 105 (2018) 424–435.
[108] X. Cai, X. Shen, L. Ma, et al., Chem. Eng. J. 268 (2015) 251–259.
[109] Y. Ren, L. Gao, J. Am. Ceram. Soc. 93 (2010) 3560–3564.
[110] M. Li, H. Wang, X. Wang, et al., Biosens. Bioelectron. 142 (2019) 111535.
[111] G. Chen, H. Wang, X. Wei, et al., Sens. Actuators B: Chem. 312 (2020) 127951.
[112] H. Wang, T. Sheng, S. Zhao, et al., Curr. Opin. Biomed. Eng. 20 (2021) 100326.
[113] E. Sehit, Z. Altintas, Biosens. Bioelectron. 159 (2020) 112165.